Direct shear behavior of concrete filled hollow steel tube shear connector for slim-floor steel beams

Emad Hosseinpour [1a], Shahrizan Baharom [*1],
Wan Hamidon W. Badaruzzaman [1b], Mahdi Shariati [2c] and Abdolrahim Jalali [2d]

[1] *Department of Civil and Structural Engineering, Faculty of Engineering and Built Environment,
Universiti Kebangsaan Malaysia, Bangi, Selangor, 43600, Malaysia*
[2] *Faculty of Civil Engineering, University of Tabriz, Bahman Blvd., Tabriz, 5166616471, Iran*

Abstract. In this paper, a hollow steel tube (HST) shear connector is proposed for use in a slim-floor system. The HST welded to a perforated steel beam web and embedded in concrete slab. A total of 10 push-out tests were conducted under static loading to investigate the mechanical behavior of the proposed HST connector. The variables were the shapes (circular, square and rectangular) and sizes of hollow steel tubes, and the compressive strength of the concrete. The failure mode was recorded as: concrete slab compressive failure under the steel tube and concrete tensile splitting failure, where no failure occurred in the HST. Test results show that the square shape HST in filled via concrete strength 40 MPa carried the highest shear load value, showing three times more than the reference specimens. It also recorded less slip behavior, and less compressive failure mode in concrete underneath the square hollow connector in comparison with the circular and rectangular HST connectors in both concrete strengths. The rectangular HST shows a 20% higher shear resistance with a longer width in the load direction in comparison with that in the smaller dimension. The energy absorption capacity values showed 23% and 18% improvements with the square HST rather than a headed shear stud when embedded in concrete strengths of 25 MPa and 40 MPa, respectively. Moreover, an analytical method was proposed and predicts the shear resistance of the HST shear connectors with a standard deviation of 0.14 considering the shape and size of the connectors.

Keywords: slim-floor; hollow steel tube; shear connector; push-out test; energy absorption capacity

1. Introduction

The slim floor system was developed in the UK as a low height and fast construction floor system (see Fig. 1). This system consists of a concrete slab placed within a steel beam to provide a flat look with lower construction costs (Chung 2002, Slim-Floor 2007). The composite action in this system is provided by the development of a web opening of a steel beam incorporating a steel rebar and concrete between the top and bottom flanges. Due to the embedded limitation of slim-floor steel beams in concrete slab, numerous techniques and arrangements of shear connectors have been proposed by researchers to promote the composite behavior of this floor system (Costa-Neves et al. 2013, De Nardin and El Debs 2012, Mangerig and Capfe 2003, Pavlović *et al.* 2013). Kuhlmann and Kürschner (2006) have proposed an inventive type of shear stud which was horizontally web-welded to the steel beam and presented a different bending behavior. The attempt to

achieve higher shear strength led to the introduction of different methods, such as using a larger size of shear stud and a welding group stud connector on the steel beam. The results recorded different types of failure mode; concrete splitting, stud welding defects, and shear stud shank failure (Lowe *et al.* 2014, Nguyen and Kim 2009, Su *et al.* 2016, Xu and Sugiura 2013, Xue *et al.* 2012). The failure of the shear stud device itself concerned researchers to introduce an alternative shear transferring mechanism such as concrete dowel and Perfobond-like. Applying reinforcement tie-bars into the web openings of the steel beam incorporating with concrete materials, shows slight improvement on shear resistance of the new shear connectors (Chen *et al.* 2015, Mangerig 2003, Limazie and Chen 2016, Classen 2015).

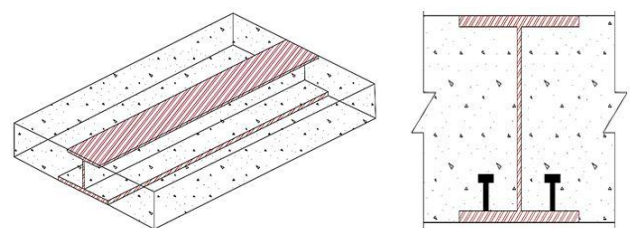Another type of shear transfer connector was introduced

∗Corresponding author, Ph.D., Senior Lecturer,
 E-mail: shahrizan@ukm.edu.my
[a] Ph.D.
[b] Ph.D., Professor
[c] Ph.D.
[d] Ph.D.

Fig. 1 Slim-floor system

by a circular web opening of the steel beam embedded in the depth of the concrete slab incorporated with a reinforced rebar passing through the openings embedded in side concrete slabs, considering the effect of the circular opening configuration on the shear strength of the connectors with/ without an additional horizontally web-welded shear stud. The concrete completely fills the steel web openings and the force flow interacts between the steel web and the infill concrete (An and Cederwall 1996, Huo and D'Mello 2013, Limazie and Chen 2017, Tsavdaridis *et al*. 2013, Vianna *et al*. 2008).

The connectors were tested under direct longitudinal shear loading, and the results indicate that a larger size of circular opening increased the ultimate shear resistance of the web-opening (WO) connectors. Even though this method improves the composite action of a slim floor system by infilling concrete up to the opening, the infilled concrete fails under direct shear force. Considerable stress develops in concrete due to the knife load produced by the thin steel beam web; such stress causes concrete to fail through crushing and cracking. This failure mechanism was demonstrated in the experimental observation of Huo (2012) and Huo and D'Mello (2013). Shear stress concentration on the steel beam web around the opening can cause the web to buckle or fracture. Tie-bar shear connectors have been proposed to strengthen WO shear connectors (Chen *et al*. 2015, Huo and D'Mello 2013). In this method, a steel rebar is placed at the center of a circular WO to bear the tensile force, thereby limiting concrete failure. However, a similar failure mode has been recorded. Therefore, placing a steel rebar at the center of infilled concrete cannot enhance direct shear resistance. Consequently, the best location of the rebar should be at the top and bottom of the infilled concrete. However, the experimental findings of Huo and D'Mello (2013) indicated that the rebar placed at the top infilled concrete failed and ruptured when punched by the steel beam web. Furthermore, the rebar at the bottom of the infilled concrete could not prevent splitting failure. Hence the HST connector is introduced to distribute shear load uniformly to the concrete area and able to transfer tensile forces without using rebar. Moreover, HST could stiffen the steel web and avoiding it from crippled and fractured. Furthermore, the installation can be done and controlled in the factory before it being transport to construction site, thus will save construction time.

Recently, the hollow steel tubes (HST) widely used as structural members due to their notable shear resistance, achieved through the composite action of the steel tubes and infilled concrete (Wang *et al*. 2016). The HSTs have been studied numerically in different shapes and sizes to investigate the shear behavior of partially encased column by Baharom and Hosseinpour (2015). The shear strength of the half hollow steel tube welded on a steel–concrete composite deck was estimated earlier through a push-out test (Uenaka and Higashiyama 2013). This type of shear connector, called a half-pipe, was welded symmetrically on the flanges of the steel beam for a conventional down stand slab system. The embedded length of the connectors in the concrete slabs was 300 mm. The variables were the diameter of the circular steel tube which was varied

between 140 mm and 165 mm. The long-embedded length of the half-pipe in the concrete slab was the cause of concrete crushing failure under applied load.

This study aimed to propose a new type of shear connector for a steel beam in a slim-floor system, called HST connectors. The connectors are using HST welded to the web opening of the steel beam which enables tube length to be embedded into the concrete slab and in filled by concrete. The various sizes and shapes of HST section available in the market were considered to determine the ideal shape for the shear connectors for the slim-floor system according to the web-opening geometry of the steel beam (Morkhade and Gupta 2015, Rodrigues *et al*. 2014). The HST shear connector could be efficient for use in steel–concrete composite beams, allowing the rebar to pass through to the concrete slabs to develop composite action (Chung *et al*. 2005, Uenaka and Higashiyama 2015). Therefore, the objective of this study is to evaluate the behavior of the HST shear connectors, considering the effect of circular, rectangular, and square geometry hollow tubes under monotonic loading. It is required to assess the performance of the HST shear connectors in comparison with the shear stud and WO connectors in the case of: ultimate load, slip behavior, separation between the steel beam and concrete slab, energy absorption, and ductility performance (Han *et al*. 2015). Finally, the shear resistance load obtained from the experiment was used to verify the test results with the currently available equation for headed studs as reference specimens, and to propose a new theoretical method to predict the ultimate shear resistance of the HST shear connector, considering the geometry effect of the sections as a novel type of shear resistance connector.

2. Experimental work

2.1 Test specimens and material properties

The specimens were made of two parts of steel and concrete materials. The steel beam was selected according to the European Code of practice (EC4 2004) from an asymmetric Universal Column (UC) section with the aim of preventing eccentric loading. The web of the steel beams comprises one opening perforated with different shapes-circular, square, and rectangular-as studied in previous research as WO shear connectors. The steel tubes were applied to the opening to form HST shear connectors (see Fig. 2), embedded in the depth of the concrete slab. The hollow tubes allow the concrete to be connected from both side of slab where it can form a continuous slab with the aim of developing a unit of composite slim floor system. The steel beam selected was UC 254 × 254 mm with 8.6 mm web thickness. The nominal yield strength and ultimate strength property of the steel beam were F_y = 420 MPa and F_u = 530 MPa, respectively. The hollow steel section properties were obtained through a coupon test, as depicted in Table 1. The total length of the tubes was considered as 132 mm, ensuring enough embedded length into the concrete slab as HST shear connectors. Different shapes of the hollow tubes, circular, square, and rectangular, were considered, as depicted in Figs. 2(a)-(c), respectively. The

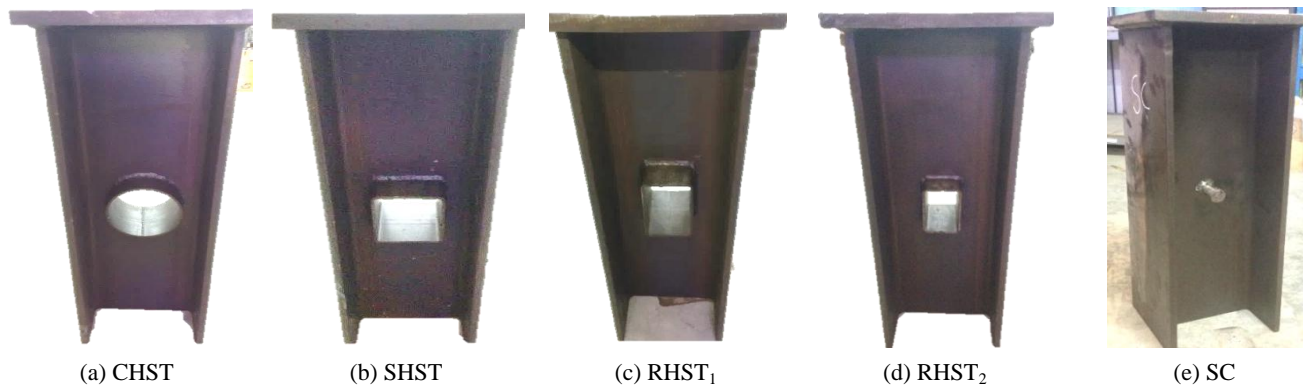(a) CHST   (b) SHST   (c) RHST$_1$ (d) RHST$_2$ (e) SC

Fig. 2 The steel beam and shear connectors

Table 1 Mechanical properties of the shear connectors measured through coupon test

Connectors	Yield strength (MPa)	Ultimate tensile strength (MPa)	Elastic modulus (MPa)	Ultimate elongation (%)
Shear stud	449.81	541.59	202.03	11.50
CHST 140	353.30	422.00	207.40	18.10
RHST$_1$ 150×100	444.00	531.70	194.00	19.90
RHST$_2$ 125×75	445.60	482.30	205.60	15.40
SHST 125×125	468.00	506.41	202.20	20.10

geometry of the tubes was considered to have the same cross-sectional area with the aim of introducing the ideal shape regarding the shear resistance of the novel connectors once filled and embedded in the concrete slab. Moreover, a smaller size rectangular HST was also considered to evaluate the effect of the dimensions on the behavior of the connectors to determine the optimum size and arrangement of the tube sections for improving the composite action of the floor system, as depicted in Fig. 2(d).

Finally, to evaluate the shear mechanism behavior of the proposed shear connectors, a standard headed shear stud with a horizontally lying arrangement was considered as the reference specimen (Kuhlmann and Kürschner 2006). In this research, varied shapes of HST shear connectors are proposed as shown in Figs. 2(a)-(d) including circular (CHST), square (SHST) and rectangular (RHST). As a benchmark specimen, the headed shear stud with 30 mm and 19 mm diameter in the head and shank, respectively, was welded symmetrically to the web post of the UC steel section on both sides, as shown in Fig. 2(e). The actual mechanical properties of each hollow steel tube section (circular, square, and rectangular) were measured through coupon tests and the average results were taken as illustrated in Table 1.

The normal strength concrete with two different strength properties of C25 and C40 as variables in this study (Table 2). The concrete slab was designed to have specimens with a total width of 800 mm and a proper length alongside the steel beam to embed the shear connectors sufficiently in the bottom and top to transfer the direct shear force to the concrete slab sides. Moreover, 50 mm at the bottom of the concrete sides was considered, to allow the steel beam section to move downward through that to enable the

vertical push-out test to transfer the load and measure the relative slip of the steel beam section through the concrete slab. The mesh rebar is commonly positioned in the concrete slab to confine the shear connectors to avoid transverse separation so as to present the real behavior of the conventional down stand composite slab under the push-out test (EC4 2004, Costa-Neves *et al*. 2013, Han *et al*. 2015, Pavlović *et al*. 2013, Xue *et al*. 2012). Since the steel beam is embedded in the depth of the concrete, the slab was placed alongside the web, encased between two flanges, so that the shear transferring mechanism of the slim-floor system is different from the down stand arrangement and there is no mesh rebar in the depth of the concrete slab around the shear connectors (Huo and D'Mello 2013). Hence, the mesh reinforcement in this study was exclusively focused on the shear resistance of the connectors alongside the web of the steel beam section subjected to the direct longitudinal force, to study the concrete splitting effect on the shear studs and the HST shear connector shear strength. However, to avoid the concrete slab crushing at the support area of push-out specimens, 10 mm diameter steel rebar hoops were applied in two layers. In addition, lifting hooks were prepared from steel rebar of 10 mm diameter and embedded on both sides of the concrete to enable the samples to be carried easily to the setup.

2.2 Specimen preparation

The mixture proportions of the different strengths of the concrete material are illustrated in Table 2, where Ordinary Portland Cement (OPC) type II was used in all mixes. The calculated value of the concrete was assumed for both sides

Table 2 The mix proportions of normal strength concrete by weight

Concrete	Cement (kg/m^3)	Coarse aggregate (kg/m^3)	Water (kg/m^3)	W/C ratio	SP (%)
C25	345	1119	746	0.55	----
C40	395	1115	700	0.48	0.5

of the specimen slabs. In order to achieve adequate workability for the concrete grade of 40 MPa, super-plasticizer Visco Crete 2055 with pH in the range of 6.0–9.0 was added to gauging water of the fresh mix at 0.5% of the cement weight (Anagnostopoulos 2014, ViscoCrete 2011). The slump of the infill concrete was increased from 50 mm to 100 mm, at which this workability finally allows the concrete to pass to the other side of the slab fill through the hollow tube section. This avoids any voids and segregation of the infill aggregate from cement paste formed in the concrete-filled HST shear connectors. The workability of the concrete mix was monitored to allow the concrete to flow and pass through the shear connectors to achieve the desired mixture proportion of aggregate (fine and coarse). Meanwhile, the concrete was compacted using an electronic vibrator machine to avoid any air voids and segregation of the infill aggregate.

To determine the compressive and tensile splitting strength of the various grades of the cast concrete, standard cube moulds with 150 mm side lengths and standard cylinders with 150 mm diameter and 300 mm length were cast at the same time as the specimens. For each concrete mix of specimens, three standard cubes and cylinders were prepared using the same batch for each sample. The compressive and tensile strength of the concrete was tested at 28 days according to the European Standard and then the results were measured to find the average for the samples. All specimens were cast in a horizontal position as is done for composite beams, and de-bonding oil was applied on the interface of the steel sections of all the test specimens with concrete to minimize the friction effect at the web of the

steel beam before casting (EC4 2004). The concrete specimens were tested at day 28, 29 and 30. Due to insignificant concrete strength increment, concrete strengths at day 28 were used.

Details of the specimens of the HST shear connectors are shown in Table 3. The first capital letters of C, S, and R in the specimen designations represent the circular, square, and rectangular types of HST section, respectively, as the variable of the shear connectors in this study. Dimensions of each hollow steel tube were measured and presented in the table. The last digit indicates the compressive strength of the concrete at 28 days, of 25 MPa (C25) and 40 MPa (C40). The two different sizes of rectangular HST shear connectors are indicated as 1 and 2, following the RHST designation system. The specimen label (SC) denotes the headed shear stud connector which was welded symmetrically on the web centre of the steel beam on both sides.

Strain gauges were positioned on the shear connectors on one side due to the symmetric geometry of the connectors in the specimens. The strain gauge installed on the top surface of the shear connectors in the loading direction, recording the compression response of the connectors, was labelled as S1#. The strain gauge in the tension area under the shear connector was labelled as S2#. The details of the test specimens and the location of the strain gauges are sketched in Fig. 3.

2.3 Push-out test setup

The push-out test was performed and carried out in accordance with EC4, in addition to which the method performed by previous researchers was adopted (Cândido-Martins *et al.* 2010, Fontana and Beck 2002, Hegger and Goralski 2004, Huo and D'Mello 2013, Xue *et al.* 2012). Besides conventional push-out tests delivering a connector strength "smeared" over several studs according to EC4, the use of single stud connector tests is gaining vital importance. These test setups have been proposed earlier by researchers (Gattesco and Giuriani 1996, Gallwoszus 2016).

Table 3 Test specimen details and concrete strength

Specimen designation	Connector type	*Connector dimension (mm)	f_{cu} (MPa)	f_{ct} (MPa)	Length of connector (mm)
SC-C25	Shear stud	Ø 19	23.39	2.33	65
SC-C40	Shear stud	Ø 19	38.00	3.30	65
CHST-C25	Circular tube	Ø 140	25.51	2.33	#132
CHST-C40	Circular tube	Ø 140	40.80	3.30	132
SHST-C25	Square tube	125×125	25.51	2.33	132
SHST-C40	Square tube	125×125	40.80	3.30	132
RHST$_1$-C25	Rectangular tube	100×150	25.51	2.33	132
RHST$_1$-C40	Rectangular tube	100×150	40.80	3.30	132
RHST$_2$-C25	Rectangular tube	75×125	25.51	2.33	132
RHST$_2$-C40	Rectangular tube	75×125	40.80	3.30	132

*The actual dimensions of HST sections were considered Ø for circular and B×H for rectangular and square geometries with 5 mm thickness

#The embedded length of the steel tube on both sides of the concrete slab through the steel web
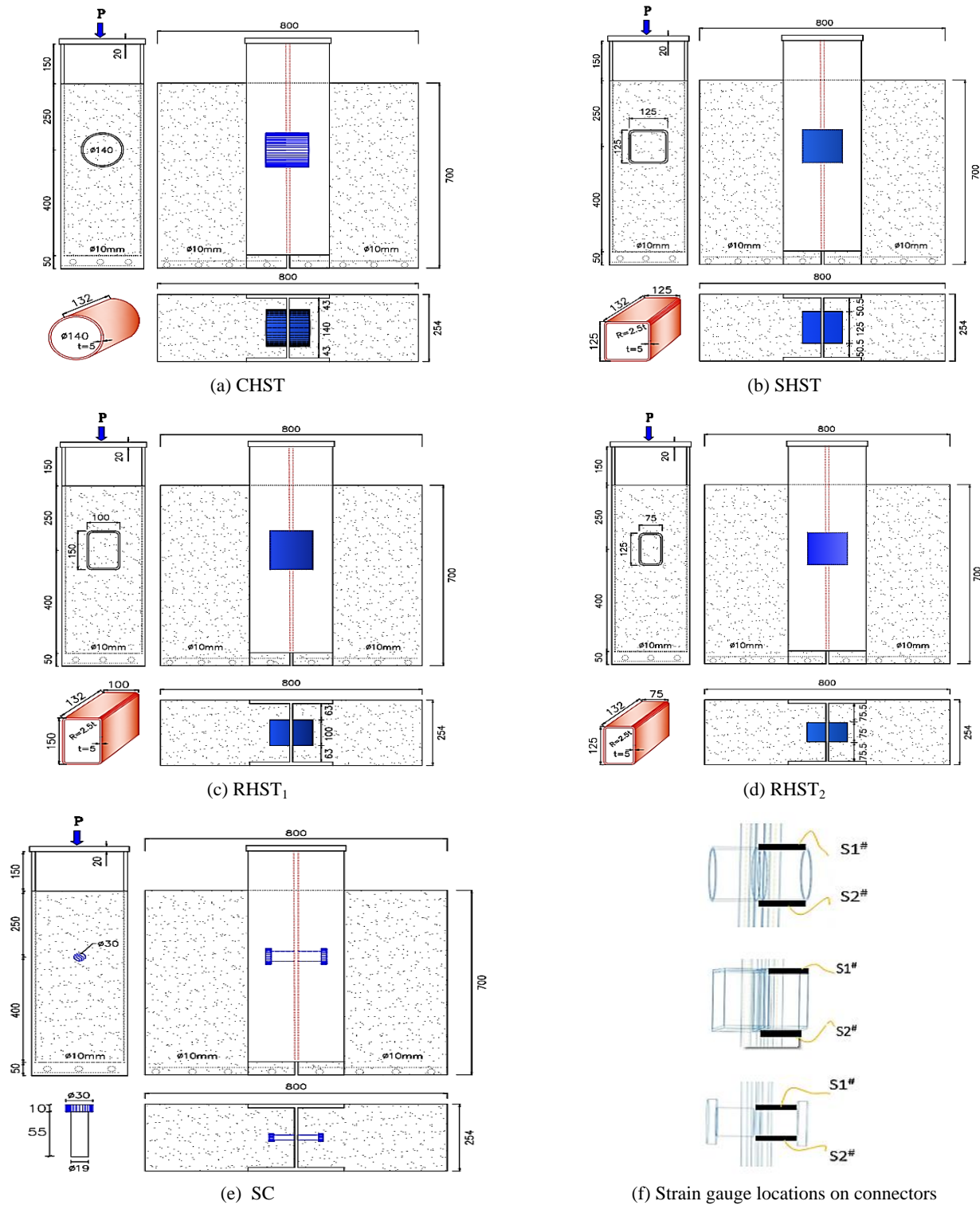
(a) CHST

(b) SHST

(c) RHST$_1$

(d) RHST$_2$

(e) SC

(f) Strain gauge locations on connectors

Fig. 3 Specimen designations and strain gauge locations

The test specimens were moved and settled vertically on four stiff steel beam supports which were located on a loading frame to prepare a strong base setup to transfer direct vertical force to the concrete slabs of the specimens to the frame. The samples were surrounded at the bottom by universal angle sections of 90 mm × 90 mm × 7 mm which were bolted together to establish the actual conditions of the concrete slabs located in the web of the slim-floor steel beam to determine the realistic behavior of the shear connectors in this system. Moreover, this prevents unwanted movement of the concrete slab due to unwanted eccentric loading on loading plate. The test setup configuration for the specimens' test series is shown in Fig. 4. A standard hydraulic actuator with 1000 kN capacity was used for direct push-out manual loading. The load–slip behavior of the connectors is usually recorded experi-
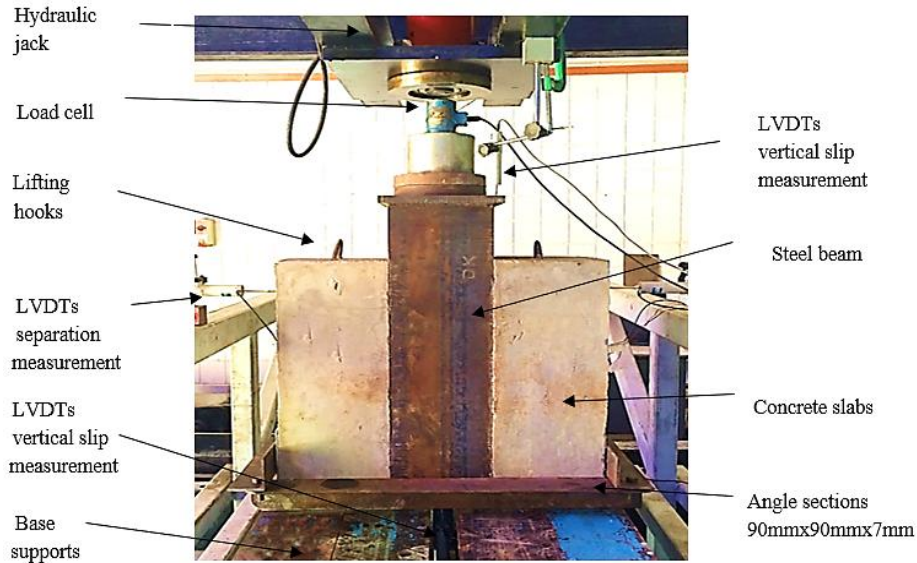
Fig. 4 Push-out test setup

mentally by both load-control and displacement-control methods (Shariati *et al*. 2013).

In this research, the tests were load-controlled with static monotonic loading which applied to the load transfer steel plate of 20 mm thickness which was welded on the steel beam section; hence, shear force was directly applied to the proposed shear connector until failure happened destructively on the shear connectors or concrete sides. To measure the slip per load in the vertical direction of the proposed shear connector, two LVDTs were positioned on the bottom of the steel beam and one LVDT was installed on top of the load transfer steel plate, which finally enabled us to determine the load–slip curves behavior of the shear connectors. Moreover, two additional LVDTs were located at 120 mm distance from the top of the concrete sides to measure the horizontal separations that occurred between the steel section and concrete on both sides. The rupture of specimens occurred suddenly in load decline with increase of the displacement by the downward movement of the steel beam section. To measure the strain deformation of the shear connectors, a strain gauge was installed symmetrically on the top (compression) and bottom (tension) zones of the HST shear connectors on the outer surface and in the shank

length of the shear stud connector as well. The specimens were cast in the structural laboratory of the National University of Malaysia (UKM). The loading rate was approximately 5 kN/minute.

3. Test results and discussion

3.1 Load–slip/separation relationships

A total of 10 push-out test samples were tested under monotonic loading. The monotonic transferred load and comparative slip for all the specimens between the steel beam section and concrete slabs were recorded stepwise by a data logger instrument. The results obtained through the installed LVDTs on the steel beam section and load cell device were drawn as load–slip behavior, while the LVDTs installed on the concrete slab recorded the load–separation relationship between steel beam and concrete slab. The slip and separation relationship of the connectors with different concrete compressive strengths of C25 and C40 were analyzed and then compared with the results obtained for the SC shear connector (solid line) to evaluate the improvement of the shear resistance of the proposed
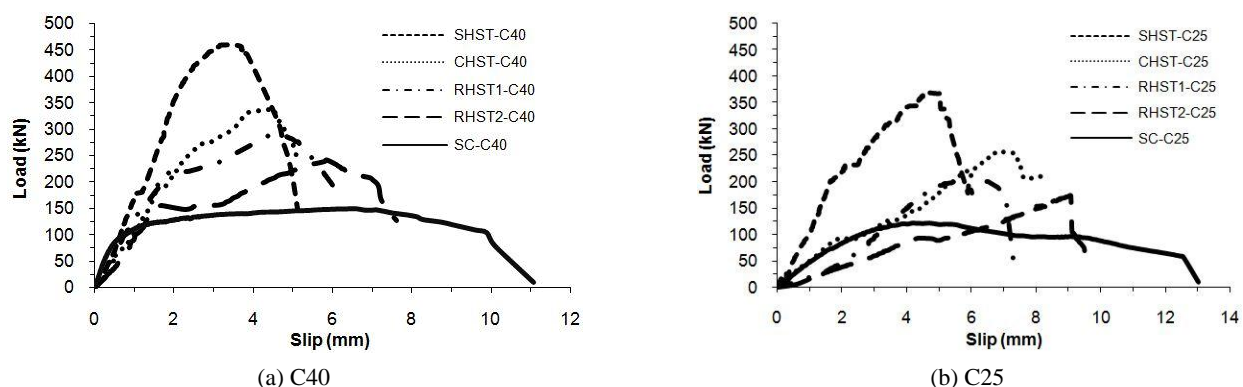

(a) C40   (b) C25

Fig. 5 Load–slip curve of the HST shear connectors compared with SC filled by concrete

connectors (see Fig. 5). The slip value was considered at the dropped load 20% below the ultimate load (EC4 2004). The results of the push-out test for the HST shear connectors show much higher shear resistance and less slip behavior in comparison with the SC specimens. The maximum slip was recorded in the SC shear connectors embedded in concrete slab of C25 with 13 mm, where the minimum slip happened in the SHST-C40 at about 5 mm. The square HST shows less slip and more shear resistance than other shapes of the HST, with 370.20 kN and 458.66 kN casting through concrete C25 and C40, respectively. The SHST-C25 shows a 45% improvement in shear resistance in comparison with CHST-C25, which carried about 258.22 kN. This also shows that CHST-C40 achieved a higher shear strength when cast by concrete C40, at about 337.93 kN, which was less effective than the SHST-C40 at about 36%.

In addition, the larger rectangular HST (RHST$_1$) shows more slip behavior (6 mm) than the CHST (5 mm), regarding concrete C40. Almost the same slip values were recorded for CHST-C25 and RHST$_1$-C25 with 7 mm, whereas, due to the less effective width of the RHST1 in the load direction in comparison with circular and square HST connectors, lower shear resistance of about 213.56 kN and 289.96 kN were recorded when infilled with C25 and C40, respectively. The highest slip values in the HST shear connectors were recorded in the smaller dimension RHST2 in the concrete strengths of both C25 and C40, with 8 mm and 10 mm slip values, respectively. The smallest effective width of RHST$_2$, rather than the other types of connectors, caused crushing through the concrete slab, with more slip behavior and lower shear resistance with ultimate load of 173.52 kN and 240.37 kN for concrete strengths of C25 and C40, respectively. However, it shows 40% and 61% improvement on the corresponding shear resistance of the SC reference specimens. Furthermore, besides increasing the shear resistance of the connection, the separation between the concrete slab and steel beam increased, as illustrated in Fig. 6 (solid line refers to the shear stud
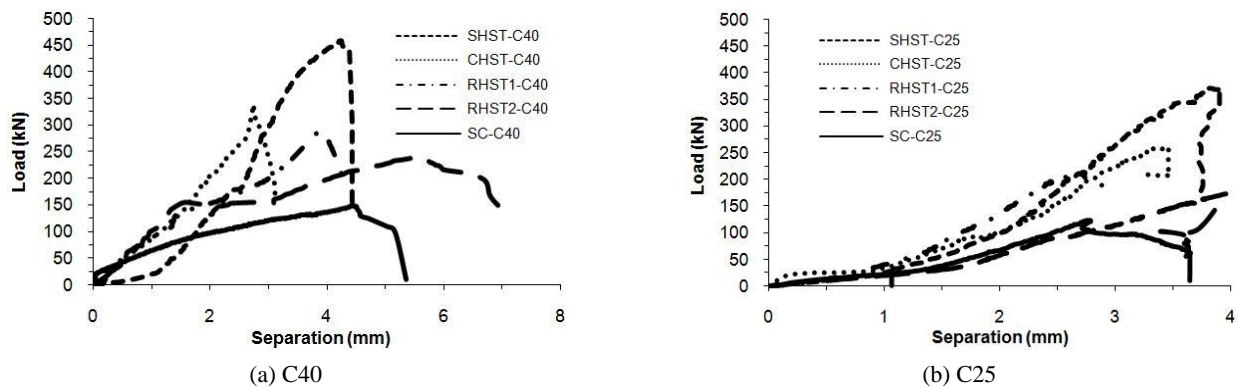

(a) C40   (b) C25

Fig. 6 Load–separation curve of the HST shear connectors compared with SC filled by concrete
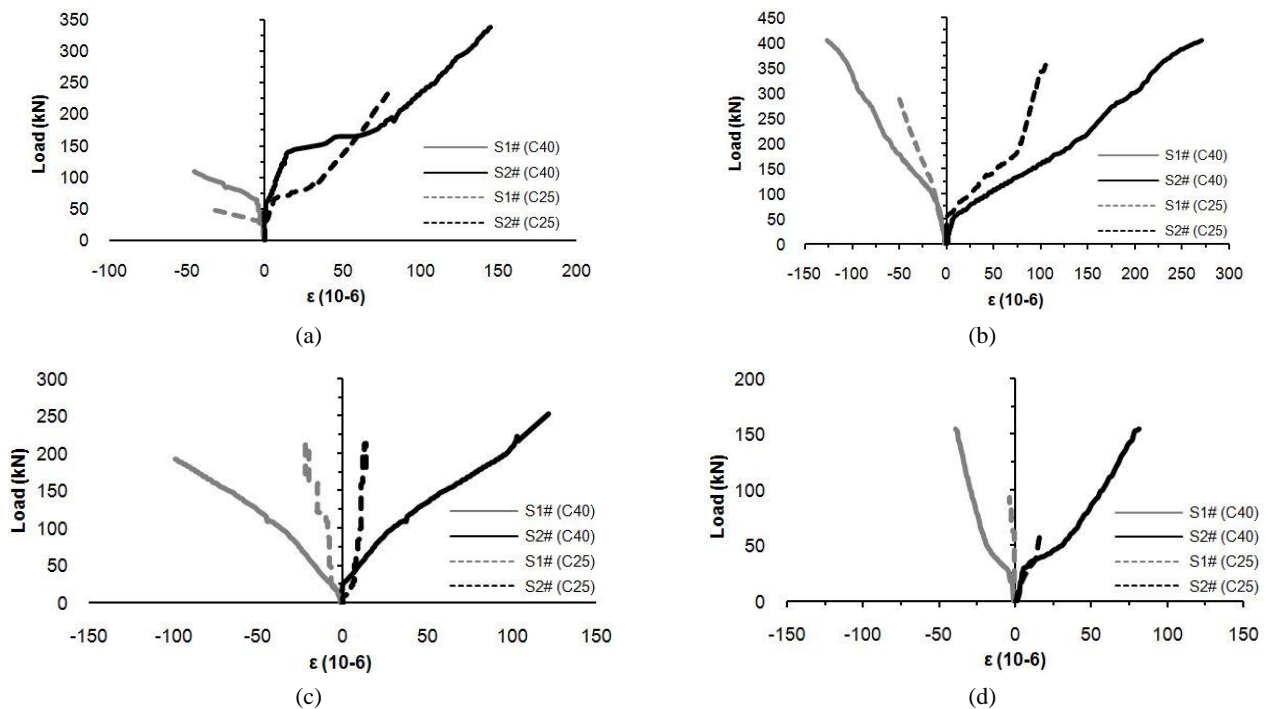

(a)   (b)

(c)   (d)

Fig. 7 The strain response of: (a) CHST; (b) SHST; (c) RHST$_1$; (d) RHST$_2$

connector). It was more obvious that the square and rectangular shape hollow connectors show more separation behavior due to the flat surface of these shapes of steel tubes interconnecting with the concrete slab, whereas the greater slip and lesser separation behavior of the CHST connector originates from the circular shape of the connector (curved shape). It can be observed that shear force is effortlessly distributed around the perimeter of the curved shape, whereas more strength and interaction behavior is shown between the concrete and the square shape, especially in the compression area and edges, which finally resulted in more separation in the SHST connector, as well as a greater shear strength behavior.

The SC connection shows more flexible behavior when the ultimate load is recorded, indicating less shear resistance and more slip behavior than the other HST shear connectors, whereas the separation behavior recorded was lower when the ultimate load was reached. The results show that the static bearing resistance of the headed shear stud embedded in both C25 and C40 concrete slab declined in contrast with the HST connectors, while the slip value of the SC increased as load was applied. The shear stud shows more ductile behavior, consisting of both elastic and plastic behavior. In the elastic stage, the load–slip curve shows an almost linear relationship, whereas in the plastic part, the slip increased rapidly, and the stiffness reduced continuously.

3.2 Load–strain relationships

According to the data recorded during testing, the installed strain gauge (see Fig. 3) started to measure strain of the HST shear connectors when the load reached 5 kN, then continued throughout the loading procedure. The strain amount by S1# recorded in "-" refers to the top part of the steel tubes under compression, while the strain data of S2# indicates the bottom part of the steel tubes under tension "+", where the unit of strain is μmm/mm or (10-6). The strain gauge in the CHST shear connection failed in the early stage of loading, whereas the strain gauge of the SHST and RHST connectors could not record the strain value in the further stage of loading. In addition, it can be seen from the load strain curves of the specimens (Fig. 7) that the strain gauges in tension failed in the further stage of loading near to the ultimate load of the test. Generally, two stages were recorded. The first stage showed the tension and compression amount as "+ -", while in the second stage the top compression strain gauge failed, and the recorded

results changed to the absolute tension strain "+". In general, the gauge did not record notable strain in the HST shear connector embedded in concrete C25, where the maximum amount of strain (270×10-6) was recorded in the SHST shear connector with infill concrete of C40, as illustrated in Figs. 7(a)-(d).

As a result, the strain gauge records in the test specimens show that the strain values of the HST connectors embedded in C25 concrete decrease to lower values than those in C40 concrete. This clearly shows that the higher slip of the HST connectors embedded in concrete C25 is because of a larger failure of the concrete underneath compared with C40 concrete. According to the great performance of the embedded infill concrete, the HST was well supported in tension and compression, so finally the strain behavior was limited to a small value for the HST shear connectors.

3.3 Failure modes

The failure mechanisms of the shear connectors were examined through the push-out test results of 10 specimens to determine the type and effective parameters that cause failure of the connectors. The failure modes of the concrete slab encased between the flanges of the steel beam via the HST shear connectors are presented in Fig. 8. Three types of failure mode were recorded in the concrete slab, whereas no failure was seen in the HST shear connectors. The failure modes consist of: concrete splitting failure, concrete cracking failure, and compressive failure of the concrete slab underneath the HST shear connectors for concrete strengths of both C25 and C40. The underneath concrete was crushed initially by the bottom flange of the HST section in the load direction, and the splitting failure cut the integration between the concrete slab and infilled concrete of the HST shear connectors in all cases (see Fig. 9). The cracking failure profiles of the concrete slab were associated with longer widths of the SHST and $RHST_1$ which increased the bearing resistance area of the concrete underneath, as presented in Figs. 9(a)-(b). The shorter effective widths of the CHST and $RHST_2$ connectors cause larger compressive failure in the concrete slab underneath in from Fig. 9(a), the effective width of the CHST shear connectors as the bearing area is less than its diameter, which resulted in compressive failure of the concrete underneath in comparison with the longer widths of the SHST and $RHST_1$.

(a) CHST   (b) SHST

Fig. 8 Typical fracture mode of concrete slab at ultimate load by the connectors
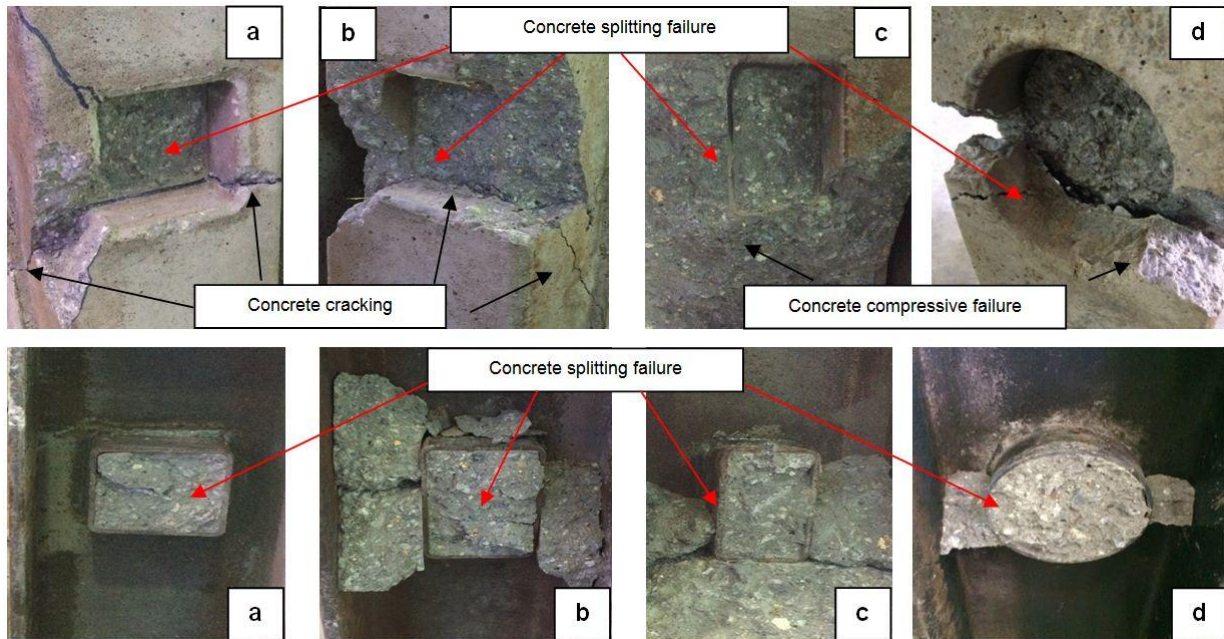
Fig. 9 Failure mode profile of the connectors: (a) SHST; (b) RHST1; (c) RHST2; (d) CHST
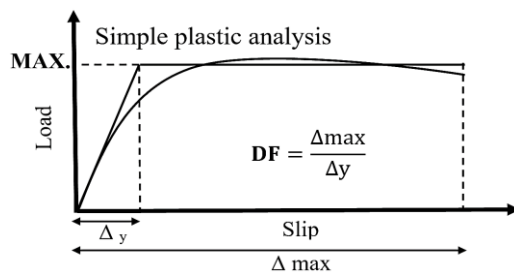

Fig. 10 Definition of ductility factor by load-slip curve (Kwon *et al*. 2011, Shariati *et al*. 2013)

Table 4 Ductility analysis of the specimen test results

Specimen	Δmax (mm)	Δy (mm)	DF
SC-C25	7.65	2.40	3.19
SC-C40	8.90	1.10	8.09
CHST-C25	7.80	5.00	1.56
CHST-C40	5.00	2.70	2.14
SHST-C25	5.34	2.85	1.87
SHST-C40	4.28	2.50	1.71
$RHST_1$-C25	7.10	4.60	1.54
$RHST_1$-C40	5.60	2.30	2.43
$RHST_2$-C25	9.10	7.50	1.21
$RHST_2$-C40	7.14	2.38	3.00

3.4 Ductility analysis

Ductility increases the safety of connections in structures before noticeable failure occurs and by letting loads be redistributed to the structural element. Through load-slip behavior of the shear connectors, evaluation of ductility performance by means of the ductility factor (DF)

is introduced by an equivalent elastic–plastic load and deflection graph, as illustrated in Fig. 10. The intersection of the two lines of the maximum load value and stiffness is considered as the yield displacement (Δy). The maximum deflection (Δmax) defines the failure point of the shear Ductility increases the safety of connections in structures before noticeable failure occurs and by letting loads be redistributed to the structural element. Through load-slip behavior of the shear connectors, evaluation of ductility performance by means of the ductility factor (DF) is introduced by an equivalent elastic–plastic load and deflection graph, as illustrated in Fig. 10. The intersection of the two lines of the maximum load value and stiffness is considered as the yield displacement (Δy). The maximum deflection (Δmax) defines the failure point of the shear connector as the load drops 10% below the ultimate load (EC4 2004), where the equivalent DF is then considered as Δmax /Δy. It can be found that a greater DF value obtained from the composite steel–concrete system represents a more ductile performance (Kwon *et al*. 2011, Shariati *et al*. 2013). The DF of the push-out test samples was then calculated and is presented in Table 4. Moreover, the shear connector's behavior can be defined ductile if the maximum slip amount is 6 mm otherwise will be specified as non-ductile, as described in EC4. Furthermore, steel-concrete composite beam should be designed as full interaction when the nonductile shear connector to be used in design while partial interaction behavior can be considered in design for ductile connector.

The slip behavior of the proposed HST connectors recorded less ductile performance than the conventional SC shear connectors in all cases of the concrete strength. This shows that the RHST2 embedded in concrete C40 recorded the highest maximum slip value together with less yield displacement, which resulted in a more ductile performance (DF = 3) than the other types of HST shear connectors, whereas the higher yield displacement value of the RHST2

with concrete C25 (7.50 mm), associated with a higher maximum slip value of 9.10 mm, resulted in the lowest DF value of all the HST test specimens. Meanwhile, the shear stud connector (SC) shows more ductile behavior with 8.09 of DF index value due to a lesser yield displacement value of 1.1 mm compared with the HST shear connectors.

3.5 Energy absorption capacity of the connectors

One way to estimate the load-carrying capability of structures under load is the energy concept. The significant concern is how to calculate the energy absorption (EA) capacity of the structures (Kazunori *et al*. 1988). The EA capacity of the tested shear connectors can be estimated by calculating the area under their load vs slip curve results (Al Zand *et al*. 2016, Arivalagan 2009). The typical procedure to estimate the area under the load–slip curves of the reference specimens (SC) and further specimens applying HST shear connectors is illustrated in Fig. 11.

The specimen cast from higher concrete strength of 40 MPa applying HST shear connectors shows a better EA capacity in the CHST and SHST shear connectors compared with the reference specimen (SC) as illustrated in Fig. 12. The SHST shear connectors have the highest energy absorption among the HST shear connectors, with 1563.83 kN.mm compared with the SC value of 1330.80 kN.mm when infilled with concrete C40, which shows an 18% improvement. The SHST-C25 recorded the highest improvement ratio of 23% compared with SC-C25 due to the higher shear resistance, almost four times greater than SC, which resulted in a larger area under the load–slip curve. The circular HST shear connectors in concrete strengths of both C25 and C40 were recorded as 1278.54 kN.mm and 1506.30 kN.mm EA capacity, which illustrates higher values than SC, with 1141.15 kN.mm and 1330.80 kN.mm, respectively. Despite the higher shear resistance

of the RHST1 and RHST2 shear connectors in comparison with SC, they show less EA capacity than SC, where RHST1-C25 and RHST2-C40 recorded the lowest EA capacity values compared with the other test specimens due to the smaller area under the load–slip curve. In general, based on the total area under the load-slip curve, the HST shear connectors specimens absorbed more energy than those with conventional headed shear stud connector which more favorable for the structural members when subjected to dynamic load such as earthquake and impact (Yousuf *et al*. 2013).

3.6 Effect of the steel tube on shear mechanism

The load transferred by the steel beam led to shear stresses on the infilled concrete as the cause of brittle failure in the WO connectors (Huo and D'Mello 2013), whereas the properties of the HST sections and their embedded length into the concrete slabs affected the shear transferring mechanism. The shear resistance of the concrete-filled HST shows improvement due to the compressive strength of the infilled concrete and the mechanical behavior of the steel tubes. This shows the notable shear resistance of the HST connector compared with the WO and SC shear connectors. The test results indicated that the infilled concrete supported the HST section to carry the shear force without any failure by supporting the internal compression and tension part of the HST connector. The compression length of the HST connector was extended, while the concrete splitting zone was shifted to inside the concrete slab in the cross-section of the HST. The advantage of using the hollow tube resulted in a better shear strength compared with the SC shear connector, where it increased the shear resistance of the SHST connector to three times more than the reference shear stud connector embedded in concrete C40, for example.
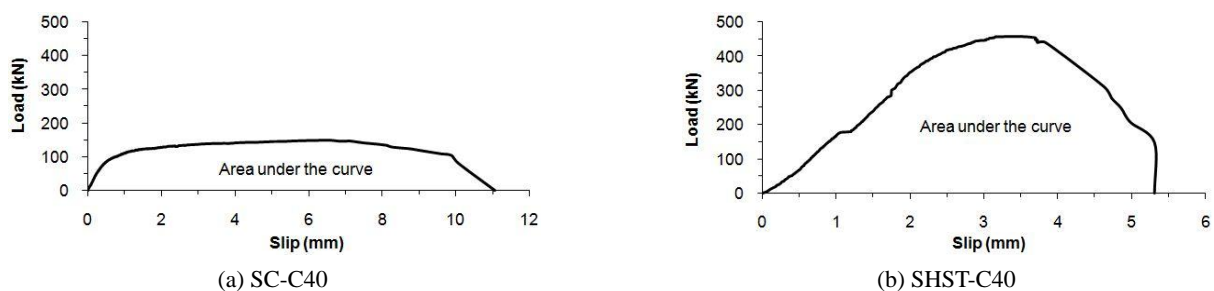

(a) SC-C40   (b) SHST-C40

Fig. 11 Typical load–slip curve to estimate energy absorption (EA) capacity

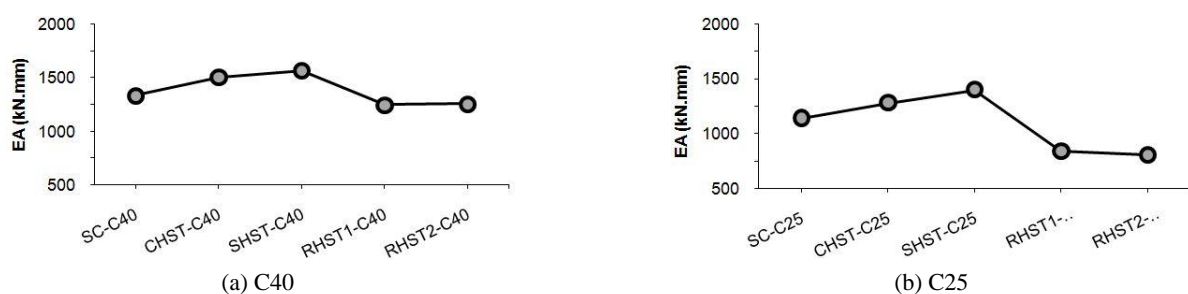(a) C40   (b) C25

Fig. 12 Energy absorption (EA) capacity of the connectors with varied concrete strength

3.7 Effect of steel tube geometry on shear strength

The shape of the HST affected the bearing resistance area of the concrete underneath the HST shear connectors. The full width of the square shape transferred the load to the concrete, whereas the effective width of the circular shape was less than its diameter (curved shape). The greatest shear resistance enhancement of the HST shear connectors was obtained by the SHST where the ultimate load shows a 36% improvement in comparison with those from CHST. In addition, regarding the two dimensions of rectangular shape shear connector, RHST1 was comparable to the CHST shear connector, whereas the RHST2 shear connector carried a shear force almost two times more than the shear stud connector. The tensile failure between the infilled concrete and concrete slab occurred in the thickness of the steel tubes, where the initial splitting started from the top edge of the HST shear connectors, and finally cracked the concrete alongside the load. Overall, the square shape connectors illustrated outstanding performance in the case of shear strength and transferring shear load to the concrete slab by full width geometry under push-out loading.

3.8 Effect of the concrete strength

The concrete material in this research affected the test results as the main parameter of the shear behavior of the connectors. The HST shear connectors, according to their contribution, were filled with concrete through the HST section allowing the side concrete slabs to be connected. In addition, the concrete-filled HST shear connectors were embedded in concrete slabs surrounded on top of and underneath the HST section in the load direction, whereas the SC as reference specimens were only embedded in concrete slabs through their length. The concrete in the HST shear connectors led to a remarkable feature for this novel type of connector by means of the concrete infilled, which increased the shear strength of the HST shear connectors. The shear transfer mechanism of the HST connectors was achieved through both compressive and tensile strength of the concrete in the underneath and filled part, respectively. This shows that the load–slip behavior of the SHST shear connector, for example, increased by 33.40% where higher concrete strength (C40) was cast, in comparison with the lower strength concrete (C25). It could be seen through the failure mode that the underneath concrete slab in the load direction plays an important role in carrying the transferred load from the concrete-filled HST shear connectors as concrete slab, where the higher compressive strength of C40 delayed the failure of the concrete slab under direct shear load in comparison with C25, which resulted in a higher shear resistance considering the compression area of the concrete slab underneath the HST shear connectors.

3.9 Shear strength of HSTs compare to headed stud

To compare the test results of HST with a single headed shear stud, the shear strength values obtained for HST were divided by two considering the embedded length of the tube in concrete slab on both sides, as illustrated in Table 5. The load improvement is the ratio of ultimate shear value between HST connectors and headed shear stud using the values obtained experimentally. The comparison indicates that the HST shear connector in all variables could carry a higher shear load than a single stud connector. The ultimate load of the circular HST connectors shows 111% and 127.24% improvement over the single headed shear stud embedded in concrete strengths of C25 and C40, respectively. The notable enhancement was achieved through the square shape of the HST connectors. The test results for SHST-C25 show 202.38% in comparison with SC-C25, while the improvement ratio increased to 208.36% for SHST-C40 compared with a single shear stud. Although, the production cost of each HST connector is higher than conventional lying stud connectors, the convincing results show that shear resistance of half side of HST connector can approximately obtain 200% more than single headed shear stud connector. Therefore, fewer number of HST connectors are needed to achieve full interaction between steel and concrete, consequently could reduce overall installation cost.

Table 5 Shear strength per HST shear connectors in comparison with single headed stud

Specimen designation	Connector length	Dimension (mm)	f_{cu} (MPa)	f_{ct} (MPa)	t (mm)	Test (kN)	Load improvement (%)
SC-C25	65.0	Ø 19	23.39	2.33	-	61.20	-----
CHST-C25	61.7	Ø 140	25.51	2.33	5	129.11	111.00
SHST-C25	61.7	125×125	25.51	2.33	5	185.06	202.38
RHST$_1$-C25	61.7	100×150	25.51	2.33	5	106.78	74.48
RHST$_2$-C25	61.7	75×125	25.51	2.33	5	86.76	41.76
SC-C40	65.0	Ø 19	38.00	3.30	-	74.37	-----
CHST-C40	61.7	Ø 140	40.80	3.30	5	169.00	127.24
SHST-C40	61.7	125×125	40.80	3.30	5	229.33	208.36
RHST$_1$-C40	61.7	100×150	40.80	3.30	5	144.98	94.94
RHST$_2$-C40	61.7	75×125	40.80	3.30	5	120.18	61.60

4. Comparison of test results with available design method for shear stud connector

The ultimate shear resistance of the headed shear stud connector achieved experimentally was evaluated with the available equation. The nominal shear strength of the stud is defined distinctly by the concrete or the stud in EC4 (2005). The shear resistance of the shear stud in EC4 is calculated as the minimum at which concrete failure or shear stud failure is presented respectively. The shear strength calculation of a single stud through EC4 shows a larger value of the shear stud than the concrete in this study, meaning that the minimum control factor is the concrete part. The experimental results obtained from the SC test series are divided by two then compared with the method suggested by EC4 per shear stud. The shear resistance for a single shear stud is calculated as 52.20 MPa with concrete grade C25 and 71.55 MPa for concrete C40, and almost the same values of the test results were achieved, with ratios of 85% and 96%, respectively.

5. Preliminary design formula for the shear strength of hollow steel tube shear connector

The shear resistance per HST shear connector can be obtained by dividing the ultimate applied load (*Pu*), as illustrated in Eq. (1).

$$Q_{u-Test} = \frac{p_u}{2} \tag{1}$$

The analytical analysis was concentrated more on the push-out test findings to establish a method to calculate the shear resistance of the HST connectors. The failure mechanism of the connectors was based on concrete splitting failure of the concrete contact surface between outer and inside tube, and compression failure of the surrounding concrete underneath the steel tube connectors as shown in Fig. 13. The effective bearing width of the circular hollow connector was recorded as 0.75D (D is
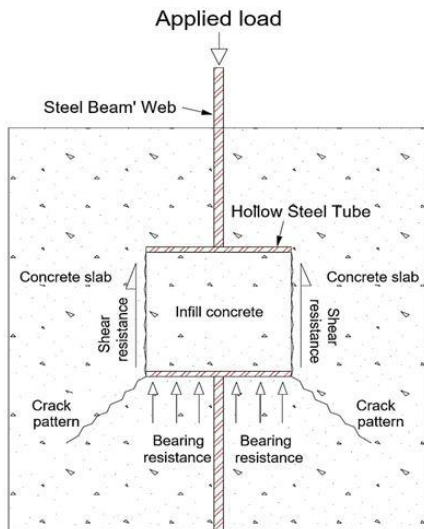

Fig. 13 Failure mechanism of HST shear connectors
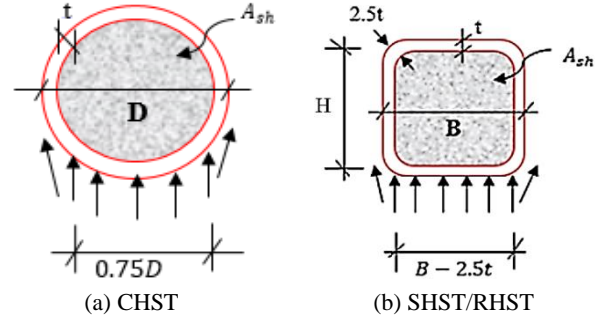

(a) CHST   (b) SHST/RHST

Fig. 14 Effective width and resistance area of the connectors

diameter) through the failure analysis of the specimens. Meanwhile, effective bearing width for SHST and RHST is taken as width of section in the direction of load excluding the curved edge. Fig. 14 illustrates the bearing area of the concrete underneath the steel tube and the shear area of the concrete slab used to estimate the shear resistance of the HST shear connectors. Eq. (2) presents an analytical calculation method to predict the shear resistance per HST connectors through the experimentally obtained results.

This method considers the bearing resistance of the concrete slab underneath the steel tubes (Q_{u-be}), besides the shear resistance of the concrete slab (Q_{u-sh}). The variables were considered based on the shape of the hollow steel tubes (circular and square/rectangular). The calculation procedure is presented through Eqs. (3)-(8), considering the coefficient factors "*a*" and "*b*" to calculate the effective bearing capacity and shear strength part of the concrete.

$$Q_{u-An} = a. Q_{u-be} + b. Q_{u-sh} \tag{2}$$

where (Q_{u-be}) is the bearing strength of the concrete underneath of the hollow steel tube, (Q_{u-sh}) is the shear resistance of the concrete infilled, "*a*" and "*b*" are the coefficients. The bearing strength of the concrete underneath of the hollow steel tube was estimated as follows

$$Q_{u-be} = A_{be}. f_{cu} \tag{3}$$

where f_{cu} is the concrete cube compressive strength in N/mm^2, and A_{be} is the bearing area of the concrete of the HST connectors in mm^2, which is defined as the effective width multiplied by the embedded length of the connector in the concrete slab.

$$A_{be} = 0.75D. L \qquad \text{Circular} \tag{4}$$

$$A_{be} = (B - 2.5t). L \qquad \text{Square and Rectangular} \tag{5}$$

The shear strength of the concrete contact surface between outer and inside tube was estimated as follows

$$Q_{u-sh} = A_{sh}. f_{ct} \tag{6}$$

where f_{ct} is the concrete tensile splitting strength in N/mm^2 and A_{sh} is the shear resistance area of the concrete infill of the hollow tubes in mm^2.

Table 6 The calculated concrete bearing and tensile strength of the HST shear connectors

Specimen designation	D or B (mm)	H (mm)	L (mm)	t (mm)	A_{be} (mm^2)	A_{sh} (mm^2)	f_{cu} (MPa)	f_{ct} (MPa)	$Q_{u\text{-}be}$ (kN)	$Q_{u\text{-}sh}$ (kN)
CHST-C25	140	-	61.70	5	6478.50	13273.23	25.51	2.33	165.3	30.9
CHST-C40	140		61.70	5	6478.50	13273.23	40.80	3.30	264.3	43.8
SHST-C25	125	125	61.70	5	6941.25	13225.00	25.51	2.33	177.1	30.8
SHST-C40	125	125	61.70	5	6941.25	13225.00	40.80	3.30	283.2	43.6
RHST$_1$-C25	100	150	61.70	5	5398.75	12600.00	25.51	2.33	137.7	29.4
RHST$_1$-C40	100	150	61.70	5	5398.75	12600.00	40.80	3.30	220.3	41.6
RHST$_2$-C25	75	125	61.70	5	3856.25	7475.00	25.51	2.33	98.4	17.4
RHST$_2$-C40	75	125	61.70	5	3856.25	7475.00	40.80	3.30	157.3	24.7
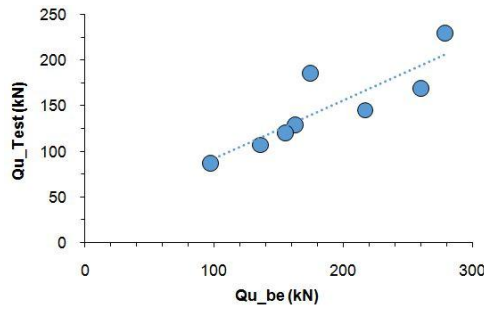
(a) Bearing strength
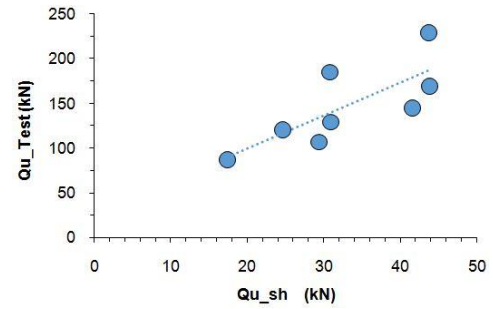
(b) Tensile shear forces

Fig. 15 The test result relationships

Table 7 Comparison of test results and analytical predicted shear resistance of HST shear connectors

Specimen	$Q_{u\text{-}Test}$ (kN)	$Q_{u\text{-}An}$ (kN)	$Q_{u\text{-}An}/Q_{u\text{-}Test}$
CHST-C25	129.1	165.3	0.99
CHST-C40	169.0	264.3	1.19
SHST-C25	185.1	177.1	0.73
SHST-C40	229.3	283.2	0.94
RHST$_1$-C25	106.8	137.7	1.01
RHST$_1$-C40	145.0	220.3	1.18
RHST$_2$-C25	86.8	98.4	0.87
RHST$_2$-C40	120.2	157.3	0.99
		MV	0.99
		SD	0.14
		COV	0.14

$$A_{sh} = \frac{\pi}{4}(D - 2t)^2 \qquad \text{Circular} \qquad (7)$$

$$A_{sh} = (B - 2t).(H - 2t) \qquad \text{Square and Rectangular} \qquad (8)$$

where D is the diameter and t is the thickness of the steel tube in mm, B and H are the width and height of the steel tube respectively in mm.

As illustrated in Table 6, the test results of the HST specimens were considered to evaluate the bearing strength and shear strength of the connectors by substituting into Eqs. (3) and (6) respectively. The findings of the equation were then normalized with the experimental results by the formation of simultaneous equations to take the sets of coefficients by solving in the multiple regression method (Fig. 15). The "a" and "b" values were obtained as $a = 0.68$ and $b = 0.50$ by considering the mean value and standard deviation of the analytical findings in comparison with the experimental test results, as illustrated in Table 7. Hence the analytical equation ($Q_{u\text{-}An}$) became Eq. (9) to predict the ultimate shear strength of the HST shear connectors.

$$Q_{u-An} = 0.68Q_{u-be} + 0.50Q_{u-sh} \qquad (9)$$

Where $Q_{u\text{-}An}$, $Q_{u\text{-}be}$, and $Q_{u\text{-}sh}$ are in kN.

The difference of the coefficients in the findings shows that the bearing strength of the concrete underneath of the HST carries most of the shear load (68%) as observed in failure mode to evaluate the shear resistance of the HST shear connectors, where only 50% of the tensile strength of the concrete resists the shear load in the push-out test.

6. Conclusions

In this research, a total of 10 push-out tests were conducted in full-scale to evaluate the shear load transfer of the HST shear connector in comparison with conventionally used headed shear studs for a Slim-Floor steel beams system. The variables considered were circular, square, and rectangular shapes of steel tube embedded in different concrete strengths of 25 MPa and 40 MPa. The results can be concluded as follows:

- The shear resistance of the HST shear connectors in both compressive strength of the concrete 25 and 40 MPa recorded higher than those conventional shear stud connectors (SC). The square HST shear connectors (SHST) carried a shear load 3 times greater than SC, which improved the direct shear performance of the Slim-Floor system by 209%. The CHST shear connectors were carried the shear resistance almost 3 times than SC, where shows less shear resistance than SHST shear connector. The shear resistance of the rectangular HST shear connectors illustrated almost 2 times more than SC. The larger bearing area of the concrete slab underneath full width of the SHST shear connectors resulted in higher shear resistance. Where, the effective bearing area of the concrete slab under CHST was less due to the curved shape.

- The ductile behavior of the SC connectors was resulted in higher slip behavior value compared with HST shear connectors. The lower concrete strength allows higher slip in all cases. The maximum slip value of the HST connectors was recorded as 10 mm, where, it was 13 mm for SC. The SHST shear connectors' shows minimum slip behavior in all cases, in contrast the $RHST_2$ connectors which were recorded higher slip values. Moreover, the largest separation between steel beam and concrete slab was recorded as 7 mm using $RHST_2$ shear connectors in contrast with 5 mm separation using SC.

- The failure mechanism of the HST shear connectors is different from that of SC. Mechanical failure of the shear stud occurred on the shank of the stud and welding zone. Concrete splitting failure around the embedded head of the shear stud was also recorded, whereas no failure happened in HST. Compressive crushing was recorded in the concrete slab underneath due to the length of the steel tube. In addition, splitting failure of the in filled concrete was noted on the perimeter of the steel tubes.

- The Ductility Factor (DF) shows the less ductile performance of the HST shear connector than SC shear specifically when embedded in concrete slab with a strength of 40 MPa. The DF index shows a higher value in SC, with 8.09 in comparison with an average of 2.3 for HST. The DF value calculated for the $RHST_2$-C25 shear connector shows the lowest ratio of 1.21, based on slip and yield displacement values of 9.10 mm and of 7.50 mm, respectively, while the highest ductility performance was recorded in the shear stud embedded in concrete C40, with a DF index of 8.09.

- The energy absorption (EA) capacity of the specimens with HST shear connectors through different strengths of the infilled concrete shows better performance in SHST shear connectors, where it achieved roughly 18% and 23% improvements in EA capacity in comparison with the SC reference specimens for the concrete strengths of C40 and C25, respectively. Further test on specimens subjected to impact load or cyclic load should be carried out to reaffirm this finding.

- The experimental results of the single SC shear connector show the same values when compared using the equation recommended by EC4. Finally, a theoretical method using multiple variable regression was developed to predict the shear resistance of the HST shear connectors. The effective coefficient factors were considered as 68% of the bearing strength of the concrete underneath the HST connectors and 50% of the tensile resistance of the concrete surface between outer and inside tube. The proposed method predicted well the shear strength of the HST shear connectors, with a mean value of 0.99 in comparison with the experimental results. The COV and standard deviation value of the prediction was 0.14 for all types of HST shear connectors, considering the circular, square, and rectangular shape steel tubes. The preliminary design formula for shear strength which developed based on empirical engineering model is capable of calculating the shear resistance of HST connectors with high accuracy. To develop on overall mechanical engineering model more insights into the real load bearing process of the HST connector are needed. A numerical parametric analysis or a larger number of tests should be performed using concrete-filled hollow steel tube shear connector to confirm the use of the proposed formula. For further study, FEA-methods can be used to analyze the local load carrying mechanisms of the connector. The analysis and derivation of design rules for connectors by systematic use of FEA can be done as explained by Classen *et al*. (2016).

References

Al Zand, A.W., Badaruzzaman, W.H.W., Mutalib, A.A. and Hilo, S.J. (2016), "The enhanced performance of CFST beams using different strengthening schemes involving unidirectional CFRP sheets: An experimental study", *Eng. Struct*., **12**(8), 184-198.

An, L. and Cederwall, K. (1996), "Push-out tests on studs in high strength and normal strength concrete", *J. Constr. Steel Res*., **36**(1), 15-29.

Anagnostopoulos, C.A. (2014), "Effect of different superplasticizers on the physical and mechanical properties of cement grouts", *Constr. Build. Mater*., **50**(1), 162-168.

Arivalagan, K. (2009), "Energy absorption capacity of composite beams", *J. Eng. Sci. Technol. Rev*., **2**(1), 145-150.

Baharom, S. and Hosseinpour, E. (2015), "Shear behavior of innovative connectors in partially encased column", *Proceedings of World Congress on Advances in Structural Engineering and Mechanics (ASEM15)*, Incheon, Korea, August.

Cândido-Martins, J.P.S., Costa-Neves, L.F. and Vellasco, P.C.G.d.S. (2010), "Experimental evaluation of the structural response of perfobond shear connectors", *Eng Struct.*, **32**(8), 1976-1985.

Chen, S., Limazie, T. and Tan, J. (2015), "Flexural behavior of shallow cellular composite floor beams with innovative shear connections", *J. Constr. Steel Res.*, **10**(6), 329-346.

Chung, K.F. (2002), "Composite beams and floor systems fully integrated with building services", *Progress in Structural Engineering and Materials*, **4**(2), 169-178.

Chung, K.F., Ko, C.H. and Wang, A.J. (2005), "Design of steel and composite beams with web openings - verification using finite element method", *Steel Compos. Struct., Int. J.*, **5**(2-3), 203-233.

Classen, M. (2015), "Shear behavior of composite dowels in transversely cracked concrete", *Struct. Concrete*, **6**(2), 195-206.

Classen, M., Herbrand, M., Kueres, D. and Hegger, J, (2016), "Derivation of design rules for innovative shear connectors in steel concrete composites by systematic use of nonlinear finite element analysis (FEA)", *Struct. Concrete*, **4**(17), 646-655.

Costa-Neves, L.F., Figueiredo, J.P., Vellasco, P.C.G.d.S. and Vianna, J.d.C. (2013), "Perforated shear connectors on composite girders under monotonic loading: An experimental approach", *Eng. Struct.*, **5**(6), 721-737.

De Nardin, S. and El Debs, A.L.H.C. (2012), Composite connections in slim-floor system: An experimental study. *J. Constr. Steel Res.*, **68**(1), 78-88.

Euro Code of practice 4 (2004), "Design of Composite Steel and Concrete Structures, part 1-1, General Rules and Rules for Buildings", European Committee for Standardization.

Euro Code of practice 4 (2005), "Design of Composite Steel and Concrete Structures, part 2, General Rules and Rules for Bridges", European Committee for Standardization.

Fontana, M. and Beck, H. (2002), "Experimental Studies on Novel Shear Rib Connectors with Powder-Actuated Fasteners", *Proceedings of Composite Construction in Steel and Concrete IV*, Alberta, Canada, April.

Gallwoszus, J. (2016), "Concrete fatigue in composite dowels", *Struct. Concrete*, **17**(1), 63-73.

Gattesco, N. and Giuriani, E. (1996), "Experimental Study on Stud Shear connectors subjected to cyclic loading", *J. Constr. Steel Res.*, **38**(1), 1-12.

Han, Q., Wang, Y., Xu, J. and Xing, Y. (2015), "Static behavior of stud shear connectors in elastic concrete–steel composite beams", *J. Constr. Steel Res.*, **11**(3), 115-126.

Hegger, J. and Goralski, C. (2004), "Structural behavior of partially concrete encased composite sections with high strength cocrete", *Proceedings of Composite Construction in Steel and Concrete V*, Mpumalanga, South Africa, July.

Huo, B.Y. (2012), "Experimental and analytical study of the shear transfer in composite shallow cellular floor beams", Ph.D. Dissertation; City University London, London, UK.

Huo, B.Y. and D'Mello, C.A. (2013), "Push-out tests and analytical study of shear transfer mechanisms in composite challow cellular floor Beams", *J. Constr. Steel Res.*, **8**(8), 191-205.

Kazunori, F., Tomonori, O. and Takashi, N. (1988), "Experimental study on energy absorption capacity of reinforced concrete frames", *Doboku Gakkai Ronbunshu*, **390**, pp. 113-121.

Kuhlmann, U. and Kürschner, K. (2006), "Structural behavior of horizontally lying shear studs", *Proceedings of 5th International Conference on Composite Construction in Steel and Concrete*, Mpumalanga, South Africa, July, pp. 543.

Kwon, G., Engelhardt, M. and Klingner, R. (2011), "Parametric studies and preliminary design recommendations on the use of post installed shear connectors for strengthening non-composite steel bridges", *J. Bridge Eng.*, **17**(2), 310-317.

Limazie, T. and Chen, S. (2016), "FE modeling and numerical investigation of shallow cellular composite floor beams", *J. Constr. Steel Res.*, **11**(9), 190-201.

Limazie, T. and Chen, S. (2017), "Effective shear connection for shallow cellular composite floor beams", *Constr. Steel Res.*, **12**(8), 772-788.

Lowe, D., Das, R. and Clifton, C. (2014), "Characterization of the splitting behavior of steel-concrete composite beams with shear stud connection", *Procedia Mater. Sci.*, **3**(1), 2174-2179.

Mangerig, I. and Capfe, Z. (2003), "Concrete dowels in composite construction", *Proceedings of Japanese-German Bridge Symposium*, Osaka, Japan, September.

Morkhade, S.G. and Gupta, L.M. (2015), "Analysis of steel I-beams with rectangular web openings: Experimental and finite element investigation", *Eng. Struct. Technol.*, **7**(1), 13-23.

Nguyen, H.T. and Kim, S.E. (2009), "Finite element modeling of push-out tests for large stud shear connectors", *J. Constr. Steel Res.*, **65**(10-11), 1909-1920.

Pavlović, M., Marković, Z., Veljković, M. and Buđevac, D. (2013), "Bolted shear connectors vs. headed studs behaviour in push-out tests", *J. Constr. Steel Res.*, **8**(8), 134-149.

Rodrigues, F., Vellasco, P.C.G.d.S., Lima, L.R.O.d. and Andrade, S.A.L.d. (2014), "Finite element modelling of steel beams with web openings", *Engineering*, **6**(13), 886-913.

Shariati, M., Ramli Sulong, N.H., Suhatril, M., Shariati, A., Arabnejad Khanouki, M.M. and Sinaei, H. (2013), "Comparison of behavior between channel and angle shear connectors under monotonic and fully reversed cyclic loading", *Constr. Build. Mater.*, **3**(8), 582-593.

Slim-Floor, A., Commercial Section (2007), http://www.arcelormittal.com/sections/

Su, Q., Yang, G. and Bradford, M. (2016), "Bearing capacity of stud–bolt hybrid shear connection in segmental composite bridge girders", *J. Bridge Eng.*, **21**(4), 06015008-1-06015008-8.

Tsavdaridis, K.D., D'Mello, C. and Huo, B.Y. (2013), "Experimental and computational study of the vertical shear behaviour of partially encased perforated steel beams", *Eng. Struct.*, **5**(6), 805-822.

Uenaka, K. and Higashiyama, H. (2013), "Experimental Study on Half-Pipe Shear Connectors Under Direct Shear", *Proceedings of Advances in Structural Engineering and Mechanics* (*ASEM*), Jeju, Korea, September.

Uenaka, K. and Higashiyama, H. (2015), "Mechanical characteristics of hollow shear connectors under direct shear force", *Steel Compos. Struct., Int. J.*, **18**(2), 467-480.

Vianna, J.D.C., Costa-Neves, L.F., Vellasco, P.C.G.d.S. and Andrade, S.A.L.d. (2008), "Structural behavior of T-Perfobond shear connectors in composite girders: An experimental approach", *Eng. Struct.*, **30**(9), 2381-2391.

ViscoCrete-2055, S. (2011), https://usa.sika.com/en/solutions _products.html

Wang, J., Afshan, S., Gkantou, M., Theofanous, M., Banioto-poulos, C. and Gardner, L. (2016), "Flexural behavior of hot-finished high strength steel square and rectangular hollow sections", *J. Const. Steel Res.*, **1**(21), 97-109.

Xu, C. and Sugiura, K. (2013), "FEM analysis on failure development of group studs shear connector under effects of concrete strength and stud dimension", *Eng. Failure Anal.*, **3**(5), 343-354.

Xue, D., Liu, Y., Yu, Z. and He, J. (2012), "Static behavior of multi-stud shear connectors for steel-concrete composite bridge", *J. Constr. Steel Res.*, **7**(4), 1-7.

Yousuf, M., Brian, U., Tao, Z., Remmenikov, A. and Richard L.J.Y. (2013), "Transverse impact resistance of hollow and concrete filled stainless steel columns", *J. Constr. Steel Res.*, **8**(2), 177-189.

CC